Direct Magneto-Optical Observation of a Structural Phase Transition in Thin Films of Manganites

V. K. Vlasko-Vlasov,[1,2] Y. K. Lin,[1] D. J. Miller,[1] U. Welp,[1] G. W. Crabtree,[1] and V. I. Nikitenko[2]
[1]*Argonne National Laboratory, 9700 South Cass Avenue, Argonne, Illinois 60439*
[2]*Institute of Solid State Physics, Chernogolovka, Russia 142432*

(Received 18 May 1999)

The spontaneous formation of twins in $La_{2/3}Ca_{1/3}MnO_3$ films below $T_S \sim 105$ K is observed by a magneto-optical technique. The twins are revealed as stripes along the {110} directions where magnetization tilts out of the film plane due to the stresses in twins. Their appearance is associated with a martensitic phase transition in the film triggered by the cubic-to-tetragonal transition in the $SrTiO_3$ substrate. It is found that magnetization of the films proceeds by inhomogeneous rotation of magnetic moments. This is due to the presence of microscopic structural inhomogeneities. Their dominating role in the low-temperature transport can explain small effects of the transition at T_S on the resistivity.

PACS numbers: 75.30.Kz, 75.30.Vn, 75.60.–d, 75.70.–i

Manganites are a unique class of materials with an extremely strong coupling between three fundamental degrees of freedom: electronic, spin, and lattice order [1]. This mutual coupling enables a rich variety of interaction effects when a change in one of the subsystems (e.g., deformation of the lattice by chemical or applied pressure) causes a response in another (such as a transition from dielectric to metallic behavior or from one type of magnetic ordering to another) [2]. One can even induce a lattice transformation by applying a magnetic field [3]. The strong coupling between subsystems drives the rich phase diagram of the manganites that includes orthorhombic (sometimes with two ortho- phases [4]), rhombohedral, and monoclinic crystal structures derived from a primitive perovskite cube and para-, ferro-, antiferro-, and canted magnetic structures, as well as metallic and insulating phases [5–7]. The mechanisms regulating the transitions between different crystallographic, electronic, and magnetic phases are still not clear and present a central challenge of the field. The double exchange interactions, which can determine magnetic ordering and conductivity in the system (both are due to the transfer of electrons between the Mn ions), give only a qualitative explanation [1]. At present most authors agree about the special role of the basic structural element: the Jahn-Teller Mn^{+3} ion surrounded by six oxygen ions. Deformations of these MnO_6 octahedra (static and dynamic) cause bending and length changes of the Mn-O-Mn bonds. This modifies the electron transfer underlying the double exchange. The same deformations produce buckling of the MnO_6 octahedra and induce structural transformations.

In thin films of manganites showing colossal values of magnetoresistance $[R(H = 0)/R(H)$ up to 10^3 [8]] the picture is even more complicated. In this case the film crystal structure may be strongly stressed as a result of film-substrate lattice mismatch [9]. Under such conditions the films may be considered as a structural modification of the bulk material with modified lattice, magnetic, and electronic properties.

In the present paper we report the observation of new magnetic structures in films of $La_{2/3}Ca_{1/3}MnO_3$ (LCMO). The structures are revealed as parallel stripes along {110} directions with magnetic moments tilted up and down from the film plane. They appear spontaneously below $T_S \sim 105$ K and do not disappear unless the sample is heated above this temperature. The magnetic stripes are associated with structural twin domains formed at $T \sim 105$ K. The appearance of twins is a regular feature of martensitic phase transformations [10] and is usually induced by transitions to a lower symmetry. In our case the film transforms from tetragonal to orthorhombic symmetry. Such a transition at T_S does not exist in bulk LCMO and is specific to the films on the $SrTiO_3$ (STO) substrates. It is triggered by the cubic to tetragonal transition in the $SrTiO_3$ substrate which occurs at nearly the same temperature. Surprisingly, resistivity measurements do not reveal any anomaly at the transition temperature. This shows that the low-T conductivity of LCMO is only slightly disturbed by the magnetic and lattice distortions produced by twins. Observations of the magnetic patterns during in-plane remagnetization reveal a strongly inhomogeneous rotation of magnetic moments, suggesting the presence of small size crystal imperfections that can be responsible for the low-T resistivity. They are especially important in manganites where the transport is spin dependent. Such defects, monoclinically distorted domains, on the scale of 10 to 100 nm, are revealed by transmission electron microscopy (TEM) observations [11,12].

The $La_{2/3}Ca_{1/3}MnO_3$ films were grown on (001) $SrTiO_3$ substrates using pulsed laser deposition. After deposition at 200–800 mTorr O_2 pressure at a substrate temperature of ~750 °C, the 1000 to 1500 Å thick films were annealed for 1 h in 700 mTorr of O2 at 750 °C. X-ray diffraction $\theta/2\theta$ scans collected from the samples at room temperature are characteristic of a textured high quality crystalline film, showing only the systematic (001) reflections with narrow rocking curves (less than ≈0.08°). Transmission electron microscopy also confirmed the film quality as well

© 2000 The American Physical Society

as the epitaxial growth of the films on the substrate. Some of the samples used in this study were deposited on bicrystalline STO substrates. The LCMO films grow on the STO substrates with their planar {100} directions turned by 45° with respect to corresponding directions in the STO substrate. This arises since the lattice constants of bulk LCMO ($x = 0.33, 293$ K) of $a = 5.4645$ Å, $c = 5.4801$ Å, and $b = 7.7722$ Å [13] match with the face diagonal of STO, $a\sqrt{2} = 3.905$ Å. The films were characterized by magnetization and 4-point resistivity measurements in fields up to 7 T. A high-resolution (down to ~ 1 μm) magneto-optical imaging technique [14] was used to map the magnetic induction component, B_z normal to the film. It is based on the Faraday rotation of the light polarization in a garnet indicator placed on the top of the sample.

Figure 1a shows a field cooled $M(T)$ curve for a 1500 Å film. It has a typical ferromagnetic form with a Curie point $T_C = 250$ K. This high value of T_C and the sharp decrease of $M(T)$ near T_C confirm the good quality of the film. The zero-field cooled (ZFC) curve first rises and then decays near T_C. Such a spin-glass-like behavior can indicate strong local distortions of magnetic moments as will be discussed later. Resistivity plots $R(T)$ (Fig. 1b) show the metal-insulator transition at T_C, which is typical for LCMO, and a considerable decrease of R in a field of 6 T. Comparison of $M(H)$ loops in fields parallel [square loop with saturation near the coercivity field (see Fig. 1c)] and normal to the film [no saturation up to 4 kG (see Fig. 1d)] reveals that the average easy axis is in the plane of the film. A small in-plane anisotropy (<100 Oe at 25 K) was observed with the minimum saturation field for $H \parallel \{100\}$ indicating that [100] and [010] are easy magnetization axes.

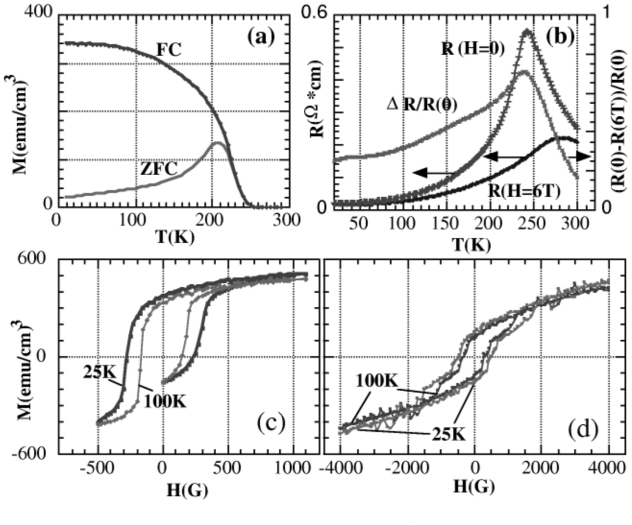

FIG. 1. (a) Temperature dependence of the magnetization at $H = 50$ Oe for field-cooled ($H \parallel$ film plane) and ZFC LCMO film. (b) Temperature changes of resistivity and magnetoresistivity (for field normal to film plane). (c), (d) Magnetization loops for in-plane and normal fields, respectively.

Figure 2a shows a magneto-optical image at 140 K in an in-plane field of 250 Oe applied along the indicated direction. Dark and bright represent negative and positive values of B_Z, and gray represents $B_Z = 0$. Thus Fig. 2a shows the magnetic pattern of an in-plane magnetized film with positive and negative stray fields emerging at the bottom and the top edges of the film, respectively. The dark line extending across the width of the sample is a grain boundary in the LCMO film by the bicrystalline substrate (37° misorientation). Here, magnetic moments are tilted out of the film plane due to stresses at the boundary. Except for the stray fields at the film edges and the grain boundary, no magnetic inhomogeneities such as magnetic domains on the scale of ≥ 1 μm were observed in any applied magnetic field. The implications of these observations for the nature of the magnetization process will be discussed below.

Below ~ 105 K a new feature appears in the magneto-optical images. Here, narrow parallel stripes of dark and bright contrast form across the entire film. These stripes are parallel to the [110] and [$1\bar{1}0$] directions of the film (in the orthorhombic *Pbnm* notation) and at 45° to {110} directions in the STO substrate. Across the grain boundary

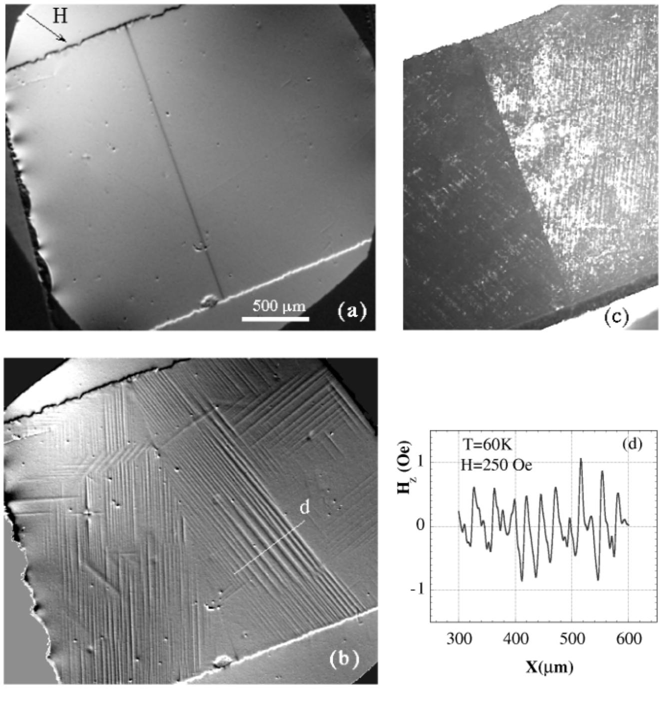

FIG. 2. Magneto-optical images (MO) of the LCMO film in the in-plane field above (a) and below (b) the transition temperature $T_S \sim 105$ K. Bright and dark reveal $\pm B_z$, and gray corresponds to B in the plane. The darkest and brightest lines near the top and bottom of the pictures correspond to stray fields at the sample edges. A dark line across the film in (a) reveals the grain boundary. (c) Twins in the substrate at $T < 100$ K (the MO indicator removed), weak contrast, and bright speckles are due to reflections from the rough bottom surface. (d) A line scan of the normal field in twins along the d line in (b).

the stripes are misoriented by the same angle of 37° as the grains of the underlying substrate. On increasing T the pattern disappears at $\sim$105 K and on successive cooling reappears again at this temperature. On different cooling cycles details of the patterns change but the orientation of the stripes remains along the $\{110\}$ axes. However, once formed the pattern does not change at lower T.

The magneto-optical contrast of the stripes depends on the applied field. It disappears at the saturating field and at the coercivity field H_C when the magnetization reversal starts. After magnetization reversal the contrast in the stripes inverts, but their positions remain fixed. Such a behavior indicates that the magnetic stripes are not magnetic domains but arise from structural elements interacting with the magnetization of the film. The most probable nature of this structure is the occurrence of twins in the LCMO film. Twins appear quite generally at martensitic phase transformations to reduce stresses arising from the lattice changes in the new low symmetry phase [10]. The orientation of twins along the $\{110\}$ directions implies that the planar $\{100\}$ axes have become unequal. Such a structural phase transition in the LCMO film arises in response to a change of the stresses to which the film is subjected. As can be seen from the room temperature lattice parameters given above, the LCMO film acquires a stretched tetragonal structure forced by the cubic STO structure [15]. This remains true at low temperatures since the thermal expansion coefficients of STO (11.1×10^{-6}) and LCMO (10.7×10^{-6} for $x = 0.33$ [13]) are essentially identical. The equilibrium structure of bulk LCMO down to 10 K, however, is orthorhombic [16]. At a temperature around 107 K STO undergoes a martensitic transition from the cubic high temperature phase to the tetragonal low-T phase [10]. This transition is accompanied by the formation of twins in the STO. In fact, images taken with the magneto-optical indicator removed show through the transparent LCMO film the occurrence of twins in the substrate that are oriented along the STO $\{110\}$ directions (Fig. 2c). It is important to note that these directions correspond to the planar $\{100\}$ directions of the LCMO film. The stripes in the film shown in Fig. 2b are, however, oriented along the LCMO $\{110\}$ directions which show that they are not a simple manifestation of the twinning in the substrate. In contrast, they represent a structural phase transition inherent to the LCMO film most likely into the equilibrium orthorhombic phase. It is brought about by the change in the stresses which in turn is caused by the transition in the substrate.

Stresses in the twin domains can tilt magnetic moments out of the film plane due to the magnetoelastic coupling. The additional anisotropy energy due to this coupling can be written as $E_A^{Tw} = -(3/2)\lambda_{ijkl}\sigma_{ij}\alpha_k\alpha_l$ where λ_{ijkl} are magnetostriction constants, σ_{ij} are twin induced stresses, and $\alpha_k = M_k/M$ are the directional cosines of the magnetization. Assuming that the magnetic moments tilt by the angle ϕ from the in-plane **x** direction towards the **z** axis normal to the film plane, $M = (M_x, M_z) = (M\cos\phi, M\sin\phi)$ and $E_A^{Tw} = -(3/2)[\lambda_{100}(\sigma_{xx}\cos^2\phi + \sigma_{zz} \times \sin^2\phi) + \lambda_{111}\sigma_{xz}\sin 2\phi]$. Accounting in the total energy E_T the in-plane anisotropy of the film $E_A = K\sin^2\phi$, the magnetostatic energy $E_{\mathrm{MS}} = 2\pi M_z^2$, and E_A^{Tw} the balance equation $\partial E_T/\partial\phi = 0$ gives the tilt value $tg 2\phi = 3\lambda_{111}\sigma_{xz}/[(3/2)\lambda_{100}(\sigma_{xx} - \sigma_{zz}) + K + 2\pi M^2]$. Accepting that stresses in twins are not very large [as is confirmed by the measured B_z values (see Fig. 2d)] we get $\phi \sim 3\lambda\sigma_{zx}/(K + 2\pi M^2)$. The tilt angle ϕ can be estimated from the locally measured values of $B_z \sim 4\pi M_z \sim 1 - 2G$ (see Fig. 2d) as $\phi \sim B_z/4\pi M \sim 10^{-3}$ (this is a lower estimate which does not account for the demagnetization effects resulting in $B_z < 4\pi M_z$). Using literature values for the anisotropy and magnetostriction constants $K \sim 10^5$ ergs/cm^3 and $\lambda \sim 10^{-5}$ [17], one obtains $\sigma_{zx} \sim 10^7$ ergs/cm^3. Thus, the observed tilts of **M** at the twins are determined mostly by relatively small out-of-plane shear stresses σ_{zx}. Such stresses are not expected in twins of a bulk sample where only in-plane components should be present.

The transition at 105 K which is clearly observed in the magnetic pattern (Fig. 2b) is hardly visible in the temperature dependence of the resistivity and magnetization. Absence of features at $M(T)$ curves is, however, more obvious. For the in-plane magnetization the changes due to the tilting are proportional to $\phi^2 \sim 10^{-6}$ which cannot be resolved. In the normal field the effect largely cancels due to the alternating signs of tilting in neighboring twins. At temperatures near 100 K the magnetoresistance has largely decayed (see Fig. 1b), implying a negligible effect on the resistivity of small tilts of the magnetic moments in twins. The absence of features in $R(T)$ at the phase transition could be due to the presence of small scale defects distributed throughout the sample that are dominating the resistivity at low temperatures. As a result, neither the transition nor the appearance of twins, spaced much wider than these defects, will strongly change the transport properties. This latter point may be inferred from details of the magnetization mechanism. As noted above, the formation of magnetic domains on the scale of >1 μm was not observed at any field implying that the remagnetization process proceeds through the rotation of magnetic moments. This is conveniently being studied by imaging the flux patterns around circular holes (see also [18]) during the in-plane remagnetization of the film (Fig. 3). The stray fields at the edges of the hole reveal values and directions of the local components of **M** normal to the edge. Except for small tilts in the twin domains **M** remains in the film plane during the field cycle. At $H \sim H_C \sim 200$ Oe the contrast at the hole edges disappears (Fig. 3b), which means that the average M turns to zero, and then inverts. Such a behavior indicates that at H_C the inhomogeneous rotation of **M** occurs incoherently in small (<1 μm) areas.

Such an inhomogeneous rotation in the film with in-plane anisotropy confirms a suggestion of numerous

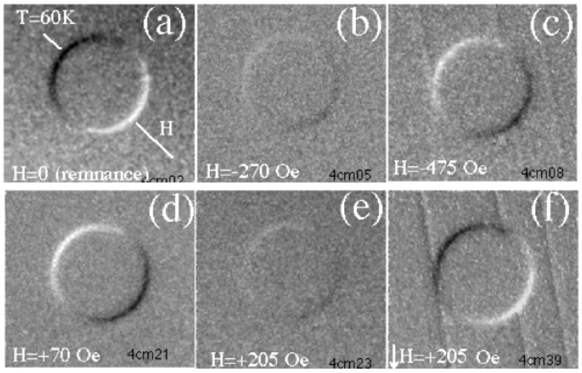

FIG. 3. Field patterns around a 100 μm hole at the in-plane remagnetization of the film. (a)–(f) follow successive points of the $M(H)$ loop [(f) at decreasing H]. The edge contrast disappears near the coercivity field [(b) and (e)] and then inverts.

microscopic imperfections in the film. Recent TEM studies of the LCMO films grown on STO by the pulsed laser deposition [11,19] revealed a columnar structure and 10 to 100 nm microdomains with differently oriented monoclinic distortions. These defects produce small lattice deformations unresolvable by x-ray diffraction. However, they can disturb magnetic moments due to the strong magnetoelastic coupling which should considerably affect the spin dependent transport in manganites. The spin-glass-like $M(T)$ curve in zero-field-cooled samples (Fig. 1a) is consistent with the above picture. Microinhomogeneities are a general feature of manganites distinguishing them from regular ferromagnets as revealed by neutron [20–22], magnetic susceptibility [23], Mossbauer [24], μSR (muon spin rotation) [25], and magnetic relaxation [26] measurements.

In conclusion, magneto-optical images reveal the appearance of twins in LCMO films on STO substrates at $T \sim 105$ K. They are associated with a martensitic transition in the LCMO film from the tetragonal to the orthorhombic phase. Such a transition is not observed in bulk LCMO and is triggered by the cubic-to-tetragonal transition in the STO substrate. The small effect of the observed structural transformation on the resistivity implies that there are other inhomogeneities, on a scale much smaller than twins, which dominate the low-T transport in manganites. Imaging of the magnetic patterns during remagnetization shows that the inversion of **M** in the film proceeds by incoherent rotation of the magnetization in microscopic areas. Structural distortions revealed by TEM can be responsible for the observed magnetic inhomogeneity in LCMO. They can also dominate the low-T resistivity.

The work was supported by the U.S. DOE, BES-Materials Sciences, under Contract No. W-31-109-ENG-38.

[1] A. J. Millis, Nature (London) **392**, 147 (1998).
[2] A. P. Ramirez, J. Phys. Condens. Matter **9**, 8171 (1997).
[3] A. Asamitsu *et al.*, Nature (London) **373**, 407 (1995).
[4] H. Kawano *et al.*, Phys. Rev. B **53**, R14 709 (1996).
[5] E. D. Wollan and W. C. Koehler, Phys. Rev. **100**, 545 (1955).
[6] Y. Tokura *et al.*, J. Appl. Phys **79**, 5288 (1996).
[7] P. G. Radaelli *et al.*, Phys. Rev. B **56**, 8265 (1997).
[8] S. Jin *et al.*, Appl. Phys. Lett. **66**, 382 (1995).
[9] C. Kwon *et al.*, J. Magn. Magn. Mater. **172**, 229 (1997).
[10] J. A. Krumhansl, in *Disorder in Condensed Matter Physics*, edited by J. A. Blackman and J. Taguena (Clarendon Press, Oxford, 1991), p. 3.
[11] C. J. Eastell *et al.*, Ceram. Trans. (to be published).
[12] R. A. Rao *et al.*, Appl. Phys. Lett. **73**, 3294 (1998); **74**, 1615 (1999).
[13] J. Blasko *et al.*, J. Phys. Condens. Mater. **8**, 7427 (1996).
[14] V. K. Vlasko-Vlasov *et al.*, in *Physics and Materials Science of Vortex States, Flux Pinning and Dynamics*, edited by R. Kossowski *et al. (*Kluwer Academic Publishers, Dordrecht, 1999), p. 205.
[15] V. S. Achutharaman *et al.*, Appl. Phys. Lett. **67**, 1019 (1995).
[16] Q. Huang *et al.*, Phys. Rev. B **58**, 2684 (1998).
[17] S. E. Lofland *et al.*, J. Appl. Phys. **79**, 5166 (1996).
[18] V. I. Nikitenko *et al.*, IEEE Trans. Magn. **33**, 3661 (1997).
[19] O. I. Lebedev *et al.*, Phys. Rev. B **58**, 8065 (1998).
[20] J. W. Lynn *et al.*, Phys. Rev. Lett. **76**, 4046 (1996).
[21] M. R. Ibarra *et al.*, J. Magn. Magn. Mater. **177–181**, 846 (1998).
[22] D. E. Cox *et al.*, Phys. Rev. B **57**, 3305 (1998).
[23] J. M. De Teresa *et al.*, Nature (London) **386**, 256 (1997).
[24] V. Chechersky *et al.*, Phys. Rev. B **59**, 497 (1999).
[25] R. H. Heffner *et al.*, Phys. Rev. Lett. **77**, 1869 (1996); Physica (Amsterdam) **230B–232B**, 759 (1997).
[26] X.-G. Li *et al.*, J. Appl. Phys. **85**, 1663 (1999).